

Supplementary Material

Estimation of groundwater age distributions from hydrochemistry: Comparison of two metamodelling algorithms in the Heretaunga Plains aquifer system, New Zealand

Conny Tschritter¹, Christopher J. Daughney², Sapthala Karalliyadda³, Brioch Hemmings³, Uwe Morgenstern³, Catherine Moore³

¹GNS Science, Taupo, New Zealand

²National Institute of Water and Atmospheric Research, Wellington, New Zealand

³GNS Science, Lower Hutt, New Zealand

Correspondence to: Conny Tschritter (c.tschritter@gns.cri.nz)

Contents of this file

Table S1: Hydrochemical parameters used in the metamodelling

Figure S1: Age distributions for samples 1-20

Figure S2: Age distributions for samples 21-40

Figure S3: Age distributions for samples 41-60

Figure S4: Age distributions for samples 61-76

Figure S5: Range in predictions from ensembles of 40 individual unchained SR and GBR

Table S2: Correspondence metrics for the 40-member ensembles of SR and GBR models

Spreadsheets (Table S3 and Table S4, attached): Input data and model results (Table S3); and time series data used for predictions, and predicted results, (Table S4)

Table S1 Hydrochemical parameters used in the metamodelling.

Abbreviation	Name	Units
Ca	Calcium	mg/L
Mg	Magnesium	mg/L
Na	Sodium	mg/L
K	Potassium	mg/L
HCO₃	Bicarbonate	mg/L
Cl	Chloride	mg/L
SO₄	Sulphate	mg/L
NO₃-N	Nitrate-nitrogen	mg N/L
NH₃-N	Ammoniacal nitrogen	mg N/L
PO₄-P	Phosphate-phosphorus	mg P/L
Fe	Iron	mg/L
Mn	Manganese	mg/L
SiO₂	Silica	mg/L
B	Boron	mg/L
F	Fluoride	mg/L
pH	pH	pH units
EC	Electrical conductivity	mS/cm at 25°C
DO	Dissolved oxygen	mg/L
T	Temperature	°C
d¹⁸O	Oxygen-18	per mil (‰)
d²H	Deuterium	per mil (‰)

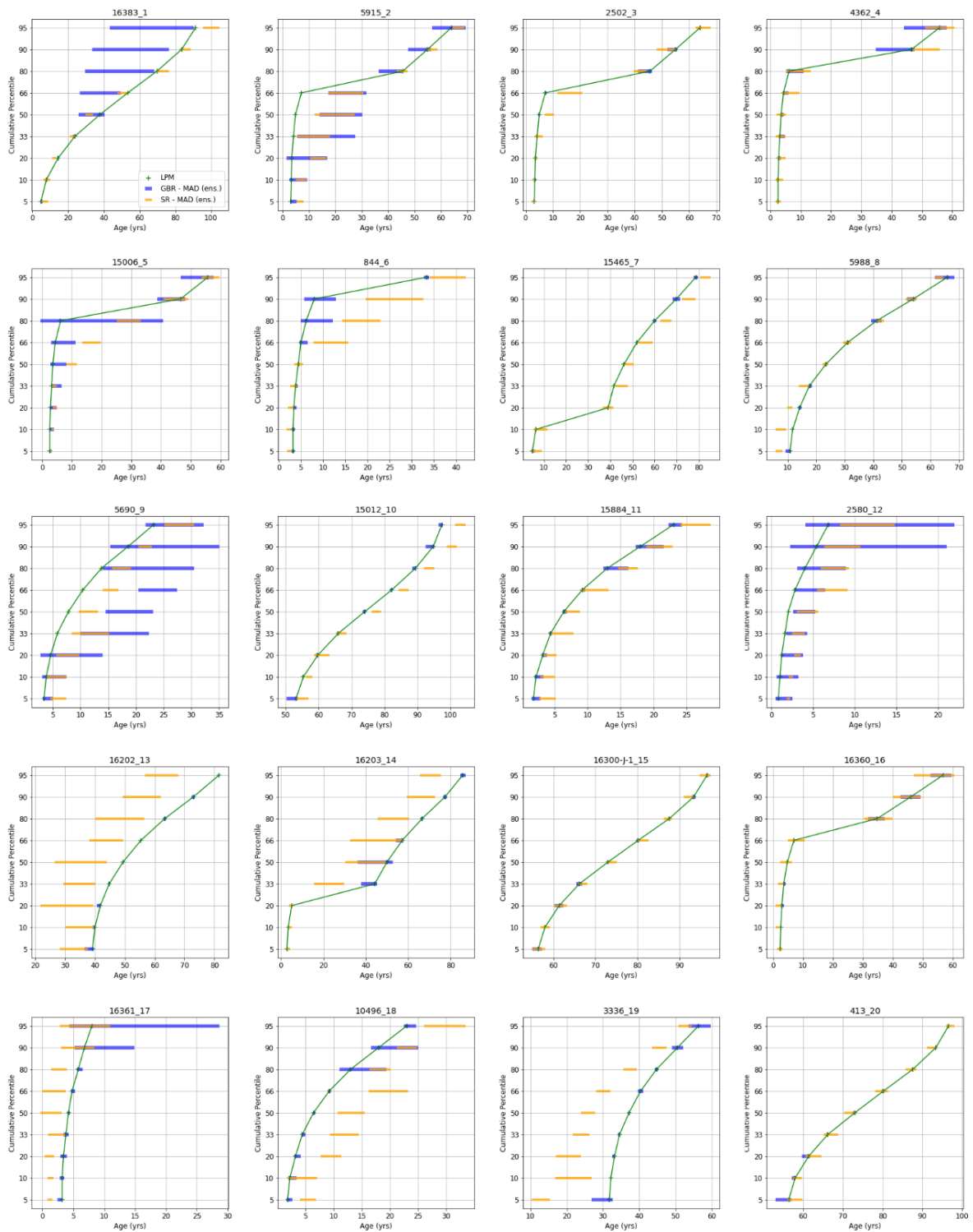


Figure S1: Age distributions for samples 1-20 based on LPMs (green) (Morgenstern et al. 2018) compared to the chained SR (orange) and GBR (blue) models developed in this study (bars represent ensemble median \pm MAD). Note, the scale of the x-axis (Age) varies between subplots. The map ID following the underscore links with the location of the site on Fig. 3.

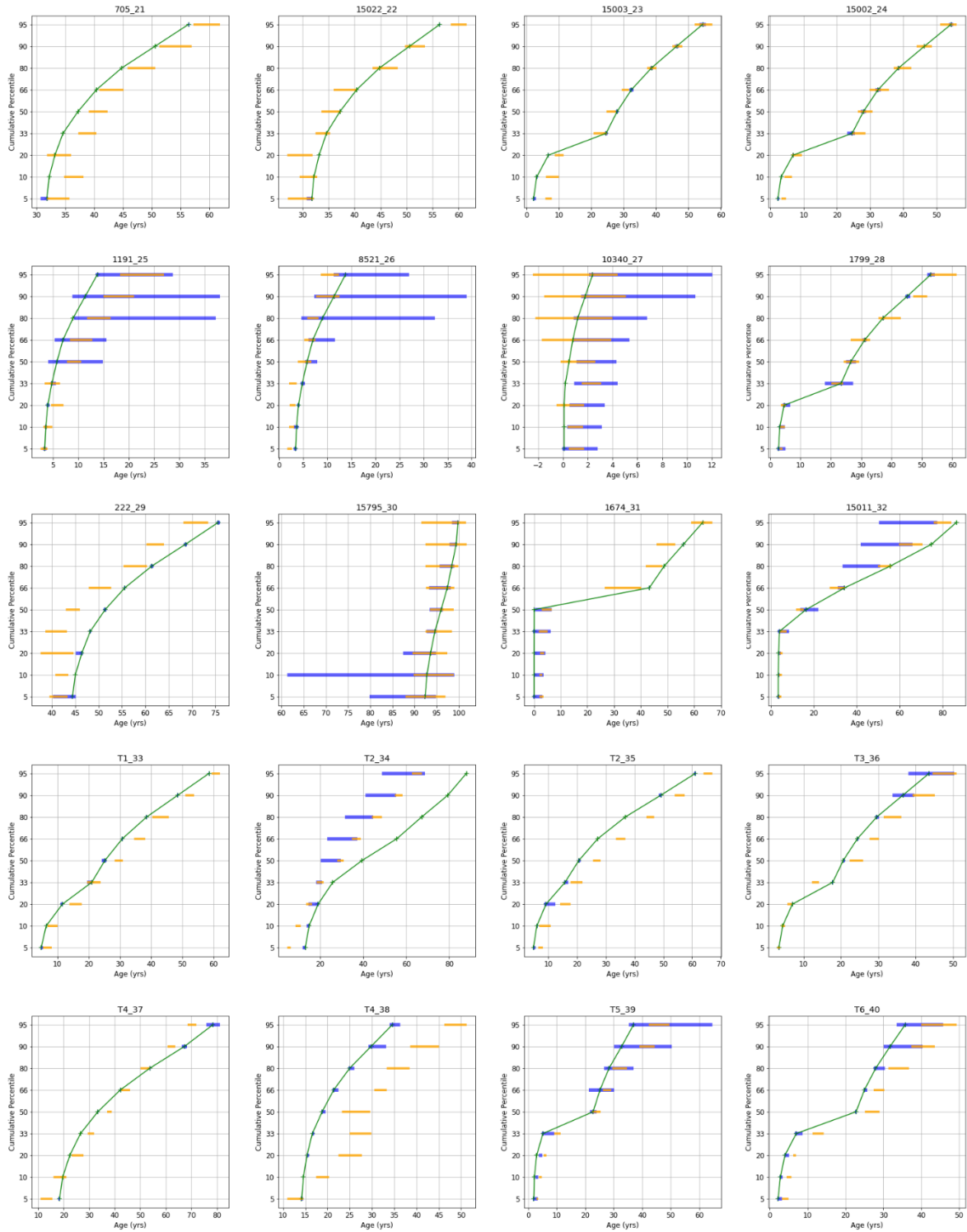


Figure S2: Age distributions for samples 21-40 based on LPMs (green) (Morgenstern et al. 2018) compared to the chained SR (orange) and GBR (blue) models developed in this study (bars represent ensemble median \pm MAD). Note, the scale of the x-axis (Age) varies between subplots. The map ID following the underscore links with the location of the site on Fig. 3.

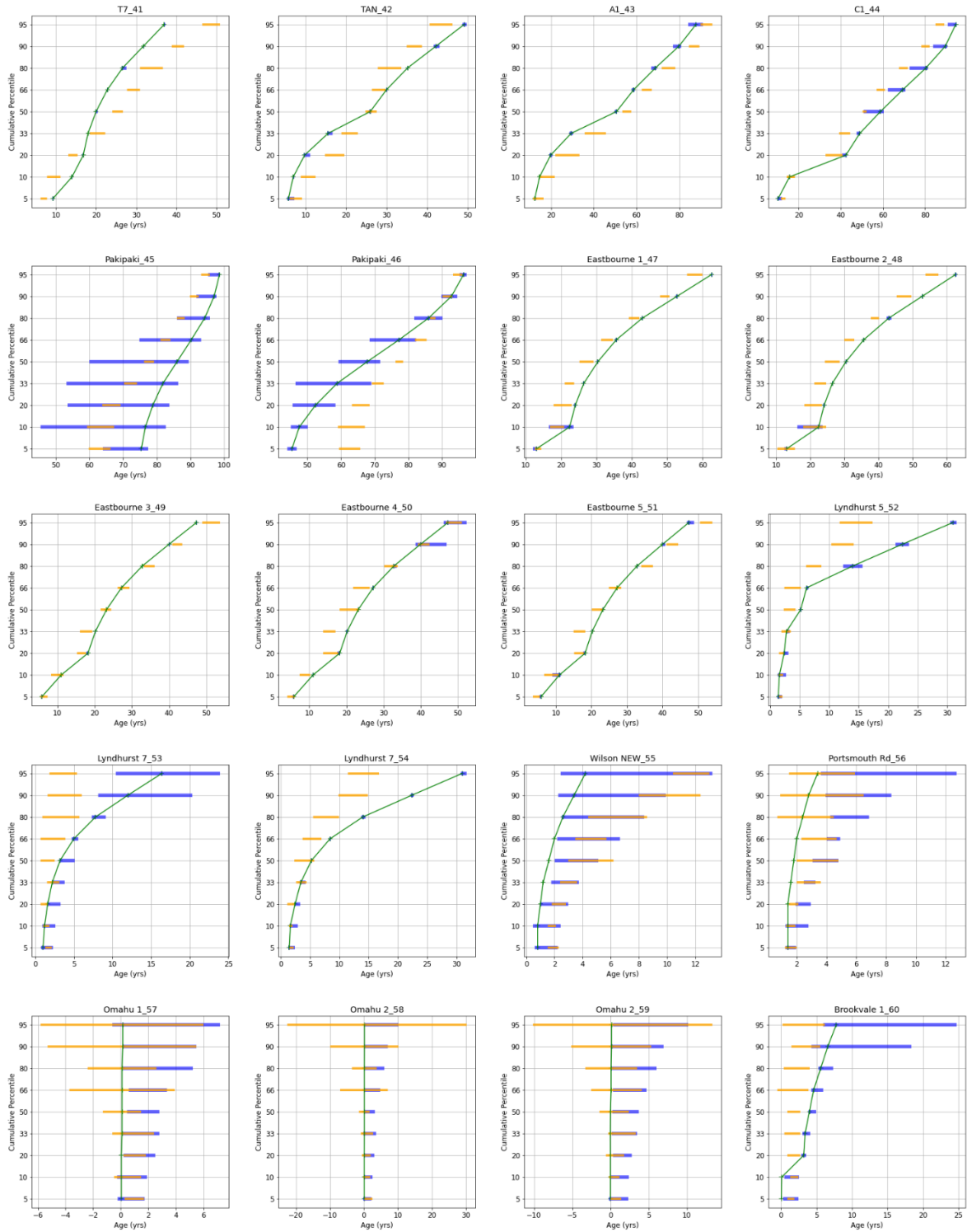


Figure S3: Age distributions for samples 41-60 based on LPMs (green) (Morgenstern et al. 2018) compared to the chained SR (orange) and GBR (blue) models developed in this study (bars represent ensemble median \pm MAD). Note, the scale of the x-axis (Age) varies between subplots. The map ID following the underscore links with the location of the site on Fig. 3.

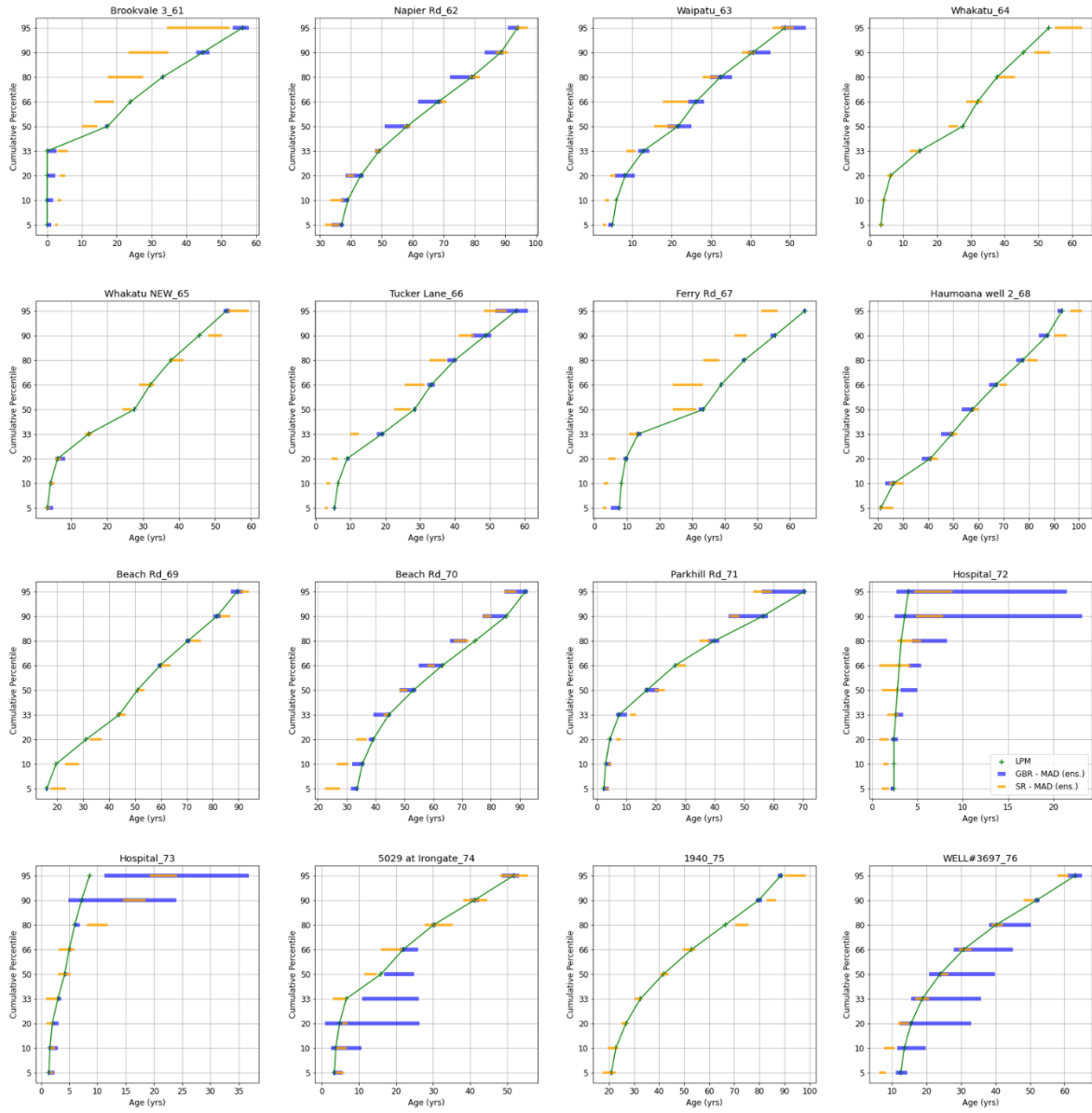


Figure S4: Age distributions for samples 61-76 based on LPMs (green) (Morgenstern et al. 2018) compared to the chained SR (orange) and GBR (blue) models developed in this study (bars represent ensemble median \pm MAD). Note, the scale of the x-axis (Age) varies between subplots. The map ID following the underscore links with the location of the site on Fig. 3.

The range in performance of the individual unchained models is illustrated for selected sites and percentiles in Fig. S5. Recall that each of the investigated percentiles was evaluated using its own suite of 40 individual models, each of which was applied to all samples in the input dataset. For all nine of the investigated percentiles and for the majority of sites, the individual unchained models produced a normal or near-normal distribution of ages with relative standard deviation of approx. 45%. However, a multi-modal distribution of age estimates was produced by model ensembles for some sites and/or percentiles, e.g. as seen with the SR for the 10th percentile at the Waipatu site (map ID 36) in Fig. S5. Moreover, for a small number of sites within the test dataset, a few of the unchained models yielded very high and inaccurate age estimates that strongly biased the ensemble average, as shown by mean ¹ median, even though the individual model's overall R² remained high. To avoid this biasing for the few cases where it occurred, we characterised the central tendency and width of each 40-member ensemble using the median and median absolute deviation (MAD) instead of the average and SD.

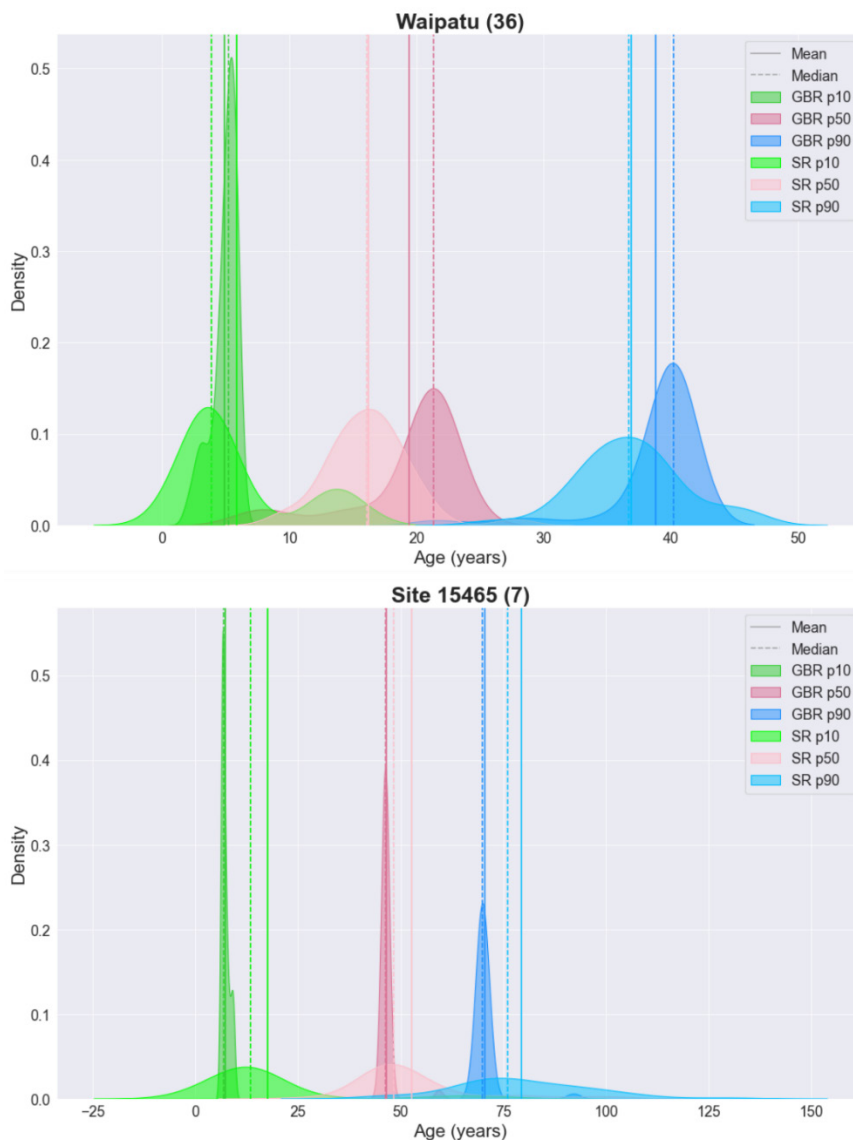


Figure S5: Range in predictions from ensembles of 40 individual unchained SR and GBR models for three different percentiles (10th, 50th and 90th) and two selected sites. Solid and dashed vertical lines indicate ensemble means and medians, respectively. Map IDs in brackets link to the location of the sites on the map in Fig. 3 of the paper.

Table S2. Correspondence metrics for the 40-member ensembles of SR and GBR models at each of nine percentiles.

	Percentile	Unchained models										Chained models									
		R ²		Absolute Error (Years)				Relative Error (%)				R ²		Absolute Error (Years)				Relative Error (%)			
		Ensemble Mean		Ensemble Mean		Ensemble Min		Ensemble Max		Ensemble Mean		Ensemble Mean		Ensemble Min		Ensemble Max		Ensemble Mean			
		Train	Test	Train	Test	Train	Test	Train	Test	Train	Test	Train	Test	Train	Test	Train	Test	Train	Test		
Symbolic Regression	5	0.88	0.77	6.2	9.0	3.3	3.4	8.7	14.5	26.5	22.5	0.97	0.88	2.4	4.8	1.3	2.9	5.7	8.1	5.8	6.3
	10	0.90	0.73	4.9	7.8	2.2	3.7	9.3	16.0	16.8	13.9	0.97	0.91	2.2	4.6	1.6	2.5	2.6	7.2	3.7	4.7
	20	0.91	0.75	4.3	6.9	2.9	3.6	6.9	11.7	6.4	8.6	0.97	0.91	2.4	4.6	1.3	2.6	4.3	6.9	3.5	5.5
	33	0.91	0.76	4.7	8.0	3.3	4.3	6.2	12.0	3.2	4.1	0.96	0.91	2.9	4.7	2.0	2.0	4.5	6.1	1.1	2.0
	50	0.92	0.77	5.2	8.7	3.7	5.5	7.6	12.5	3.4	5.4	0.96	0.92	3.2	5.1	2.2	3.7	4.9	6.6	1.5	2.6
	66	0.89	0.73	6.4	10.0	4.8	6.6	9.5	13.7	1.8	3.4	0.95	0.89	3.9	6.5	2.5	4.7	5.2	8.9	1.0	2.2
	80	0.87	0.72	7.3	11.6	5.7	6.9	10.7	16.3	2.2	2.4	0.95	0.88	4.2	7.3	2.8	4.6	5.2	10.2	0.9	3.0
	90	0.85	0.65	8.1	13.7	6.0	11.6	11.5	16.4	1.7	3.6	0.94	0.88	4.9	7.9	3.5	5.8	7.0	10.3	0.6	2.2
	95	0.84	0.62	8.6	15.4	6.4	10.8	11.6	19.9	1.8	4.5	0.93	0.87	5.4	8.9	3.9	6.4	7.3	11.9	0.6	3.1
AI	1	0.83		7.5						7.3		0.94		4.4						2.6	
Gradient Boosted Regression	5	0.99	0.76	1.04	5.32	0.00	0.05	4.75	31.8	4.17	7.02	1	0.51	0.44	7.69	0.01	0.05	2.69	43.8	2.42	6.48
	10	1	0.76	0.48	5.28	0.00	0.04	2.04	31.0	2.52	7.35	1	0.53	0.43	8.24	0.00	0.02	2.80	41.6	2.82	6.90
	20	1	0.82	0.47	5.48	0.00	0.09	2.05	34.2	2.82	7.42	0.99	0.70	0.71	7.34	0.00	0.03	8.29	34.5	3.60	7.54
	33	1	0.81	0.37	6.43	0.00	0.05	1.64	27.5	0.47	3.51	0.98	0.78	1.13	7.03	0.00	0.04	11.92	28.8	1.21	4.72
	50	1	0.80	0.20	7.37	0.00	0.19	0.59	26.3	0.19	4.81	0.98	0.79	1.41	7.65	0.00	0.19	16.88	28.1	1.87	6.23
	66	1	0.81	0.18	8.43	0.00	0.01	0.51	24.9	0.06	2.04	0.97	0.80	1.61	8.41	0.00	0.17	25.40	28.0	0.62	1.80
	80	1	0.82	0.34	8.86	0.00	0.07	0.85	24.6	0.15	2.15	0.96	0.80	2.11	9.42	0.00	0.09	29.12	31.7	0.78	2.26
	90	1	0.73	0.30	11.09	0.00	0.43	1.05	39.8	0.14	1.72	0.95	0.78	2.67	10.20	0.00	0.14	31.25	39.7	0.57	1.93
	95	1	0.74	0.41	12.18	0.02	0.36	1.02	29.78	0.13	1.90	0.96	0.77	2.66	10.19	0.00	0.58	29.22	49.2	0.65	2.12
AI	1	0.98		1.16						1.47		0.95		2.16						1.90	